# Detecting a forced signal in satellite-era sea-level change

Kristin Richter, Benoit Meyssignac, Aimée B. A. Slangen, Angélique Melet, John A. Church, Xavier Fettweis, Ben Marzeion, Cécile Agosta, Stefan R. M. Ligtenberg, Giorgio Spada, et al.

HAL Id: insu-03706465

https://insu.hal.science/insu-03706465

Submitted on 28 Jun 2022

**LETTER • OPEN ACCESS**

# Detecting a forced signal in satellite-era sea-level change

To cite this article: Kristin Richter *et al* 2020 *Environ. Res. Lett.* **15** 094079

View the article online for updates and enhancements.

# Environmental Research Letters

**LETTER**

# Detecting a forced signal in satellite-era sea-level change

Kristin Richter[1,2,15] ⓘ, Benoit Meyssignac[3] ⓘ, Aimée B A Slangen[4], Angélique Melet[5], John A Church[6], Xavier Fettweis[7], Ben Marzeion[8], Cécile Agosta[7], Stefan R M Ligtenberg[9], Giorgio Spada[10], Matthew D Palmer[11] ⓘ, Christopher D Roberts[12] and Nicolas Champollion[13,14]

1  Institute for Atmospheric and Cryospheric Sciences, Universität Innsbruck, Austria
2  NORCE Norwegian Research Centre, Bjerknes Centre for Climate Research, Bergen, Norway
3  LEGOS, Université de Toulouse, CNES, CNRS, IRD, UPS, Toulouse, France
4  Department of Estuarine and Delta Systems, Royal Netherlands Institute for Sea Research, Yerseke, The Netherlands
5  Mercator Ocean, Ramonville St Agne, France
6  Climate Change Research Centre, University of New South Wales, Sydney, NSW 2052, Australia
7  Department of Geography, University of Liège, Liège, Belgium
8  Institute of Geography, University of Bremen, Bremen, Germany
9  Institute for Marine and Atmospheric Research Utrecht, Utrecht University, Utrecht, The Netherlands
10 University of Urbino, Urbino, Italy
11 Met Office Hadley Centre, Exeter, United Kingdom
12 European Centre for Medium Range Weather Forecasts, Reading, United Kingdom
13 Institut des Géosciences de l'Environnement, CNRS, IRD, Univ. Grenoble Alpes, Grenoble, France
14 Bern International Space Science Institute, Hallerstrasse 6, 3012, Bern, Switzerland
15 Author to whom any correspondence should be addressed.

**E-mail:** krri@norceresearch.no

## Abstract

In this study, we compare the spatial patterns of simulated geocentric sea-level change to observations from satellite altimetry over the period 1993–2015 to assess whether a forced signal is detectable. This is challenging, as on these time scales internal variability plays an important role and may dominate the observed spatial patterns of regional sea-level change. Model simulations of regional sea-level change associated with sterodynamic sea level, atmospheric loading, glacier mass change, and ice-sheet surface mass balance changes are combined with observations of groundwater depletion, reservoir storage, and dynamic ice-sheet mass changes. The resulting total geocentric regional sea-level change is then compared to independent measurements from satellite altimeter observations. The detectability of the climate-forced signal is assessed by comparing the model ensemble mean of the 'historical' simulations with the characteristics of sea-level variability in pre-industrial control simulations. To further minimize the impact of internal variability, zonal averages were produced. We find that, in all ocean basins, zonally averaged simulated sea-level changes are consistent with observations within sampling uncertainties associated with simulated internal variability of the sterodynamic component. Furthermore, the simulated zonally averaged sea-level change cannot be explained by internal variability alone—thus we conclude that the observations include a forced contribution that is detectable at basin scales.

## 1. Introduction

During the altimetry period (1993–2018) global mean sea level (GMSL) has been rising at a rate of about 3 mm yr$^{-1}$ (WCRP Global Sea Level Budget Group 2018). This is about double the rate of 20th century GMSL rise, depending on the tide-gauge based reconstructions used (Church and White 2011, Ray and Douglas 2011, Jevrejeva *et al* 2014, Hay *et al* 2015, Dangendorf *et al* 2017, 2019, Oppenheimer *et al* 2019). The observed GMSL rise inferred from satellite altimetry (Dieng *et al* 2017, Legeais *et al* 2018) agrees with the sum of the observed contributions (WCRP Global Sea Level Budget Group 2018), as well as with the sum of simulated contributions from CMIP5 climate models (Slangen *et al* 2017).

Over the altimetry period, GMSL rise is about 40% due to thermal expansion (i.e. 'global-mean thermosteric sea-level rise') and 60% due to mass contributions (changes in land ice and terrestrial water storage, i.e. 'barystatic sea-level rise') (WCRP Global Sea Level Budget Group 2018, Gregory *et al*

2019). The spatial pattern of change, however, is mainly related to ocean dynamic sea-level change, which dominates over the barystatic fingerprints (e.g. Spada and Galassi 2016) that result from changes in Earth gravity, rotation and viscoelastic solid-Earth deformation (GRD, Gregory *et al* 2019) due to shrinking land ice from glaciers and ice sheets as well as changes in terrestrial landwater storage.

Several studies have shown that the total GMSL change (Dangendorf *et al* 2015, Slangen *et al* 2016) as well as the component contributions (Marcos and Amores 2014, Slangen *et al* 2014, Marzeion *et al* 2014) are partly driven by external climate forcings (e.g. increasing greenhouse gas concentrations). These studies usually consider time periods of at least 40 years or more. Detecting a forced trend in sea level becomes more challenging on smaller space- and shorter time-scales as regional modes of internal variability have a larger influence on sea level at these scales. Here, we refer to *internal variability* as sea-level changes originating from inherent climate variability, particularly in the coupled ocean-atmosphere system. This includes climate modes such as El Nino-Southern Oscillation (ENSO), Pacific Decadal Oscillation and North Atlantic Oscillation (e.g. Roberts *et al* 2016). Conversely, a *forced signal* is related to external drivers, both natural (e.g. volcanic eruptions) as well as anthropogenic (e.g. greenhouse gas emissions).

The large contribution of internal variability in sterodynamic sea-level change (changes in ocean density and circulation) complicates the detection of a forced regional sea-level signal on decadal time scales. Richter *et al* (2017) showed that extensive spatial averaging is necessary to detect a forced signal in sterodynamic sea-level change for period lengths similar to the altimetric record (i.e. 25 years). To assess whether a forced signal can be detected regionally in total sea level over this short period of time, we compare the simulated total sea-level trend patterns with the observed trends from altimetric observations over the period 1993–2015 while also taking simulated internal variability into account.

The dataset used in our analysis originates from two recent studies that compared global and regional sea-level change as observed and derived from tide gauges with model-simulated changes over the 20th century (Slangen *et al* 2017, Meyssignac *et al* 2017a) Meyssignac *et al* (2017a) showed that observed (coastal) multidecadal variability is well reproduced by the model ensemble and mainly originates from the sterodynamic sea-level contribution. We will therefore focus on the sterodynamic contribution when quantifying internal variability.

## 2. Data and methods

The data sets used in this study are described in detail by Slangen *et al* (2017) and Meyssignac *et al*

(2017a). This section summarizes the most important methodological details. Regional sea-level change was estimated using output from 12 climate models (supplementary material, table 1) contributing to phase 5 of the Climate Model Intercomparison Project (CMIP5, Taylor *et al* 2012) over the period 1900–2015. The output of the climate model simulations was used to calculate the components of sea-level changes associated with sterodynamic sea level, atmospheric loading, glacier mass changes, and ice-sheet surface mass balance contributions. The contribution from groundwater depletion, reservoir storage, and dynamic ice-sheet mass changes was estimated from observations as they are not simulated by climate models.

Annual mean values were computed from the monthly mean output from CMIP5 historical simulations (1993–2005 here) and the Representative Concentration Pathway 8.5 scenarios (RCP8.5, 2006–2015). The choice of CMIP5 scenario and models was based on maximum data availability to ensure a consistent model dataset. We note that RCPs remain similar during the first part of the 21st century, and our results are not sensitive to the choice of RCP.

Ocean dynamic sea level was taken directly from the CMIP5 models. As most models employ the Boussinesq approximation and conserve volume rather than mass, the global mean was removed from those fields. Global-mean thermosteric sea-level change was then obtained from integrating the three-dimensional temperature field using the United Nations Educational, Scientific and Cultural Organization (UNESCO) 1980 international equation of state (IES80). Combining dynamical sea level with the global thermosteric change gives the total sterodynamic sea-level change.

Changes in atmospheric mass and surface pressure distribution result in regional sea-level changes. Those changes have been computed using CMIP5 data, following Stammer and Hüttemann (2008). Though small over most of the ocean area, they can make a significant contribution regionally.

Glacier mass change and the SMB contribution from the ice sheets are derived from model output as follows. The glacier model by Marzeion *et al* (2012) is forced with CMIP5 temperature and precipitation to model the SMB of the worlds glaciers while taking changes in hypsometry into account. Greenland SMB is computed by forcing the regional climate model MAR with CMIP5 temperature and precipitation from the extended historical CMIP5 simulations (Fettweis *et al* 2013, Meyssignac *et al* 2017b). The Antarctic SMB is computed as the average of two estimates: the first method approximates the SMB from the CMIP5 change in precipitation minus evaporation in each model over the Antarctic ice sheet, scaled to fit the best estimate of the Antarctic SMB for the period 1985–2010 from the regional climate model RACMO2.1 forced by ERA-Interim

reanalysis data (Lenaerts *et al* 2012). The second method assumes a linear relationship between the SMB change and CMIP5 Antarctic surface temperature of 6% K$^{-1}$, consistent with observations of the last deglaciation based on ice-core data (Frieler *et al* 2015). Both methods yield similar results over the 20th century.

For the contribution from ice-sheet mass changes due to dynamic ice flow, we use the estimate by Shepherd *et al* (2012) from 1992 to 2011. The ice dynamical time series are then extended to 2015 using the assumption that the West Antarctic discharge was slightly above the 2008–2012 average (Sutterley *et al* 2014) according to a constant mass loss rate, the East Antarctic and Antarctic Peninsula discharge followed the 2001–2010 average, and the Greenland ice sheet discharge was constant at the 2010 value (Enderlin *et al* 2014).

As with the dynamical ice-sheet mass change, the sea-level contribution from groundwater depletion and reservoir storage is not represented in the climate models used in this study and is therefore based on observations. The groundwater contribution was taken from Döll *et al* (2014), while the contribution from artificial reservoirs was taken from Chao *et al* (2008). The latter data was available until 2008. The average rate of the last 5 years of available data was used thereafter to extend the data to 2015.

The regional sea-level changes associated with the transfer of mass between ocean and land described above (i.e. changes in land ice and landwater storage) were computed using the average of two different sea-level equation solvers. One is based on an updated version of SELEN (Spada *et al* 2012) and the other one on Schotman (2008). Both include the effects of Earth rotation. In contrast to Slangen *et al* (2017) and Meyssignac *et al* (2017a), geocentric instead of relative GRD fingerprints were computed in order to compare modelled sea level with altimetric (geocentric) sea level.

Lastly, we account for the ongoing response of the sea surface to the last deglaciation (glacial isostatic adjustment, GIA). As before, we are interested in geocentric instead of relative sea-level changes. Therefore, we only include the present-day rate of sea-surface variation (e.g. Tamisiea 2011, Spada 2017) as provided by Peltier (2004). The model uses the ICE-5G ice chronology and includes the feedback on sea level caused by Earth rotation. Note that the GIA-related geocentric sea-level trend patterns are very different from their relative sea-level counterpart (compare e.g. Figures 2(a) and (c) in Spada 2017) with opposite sign in regions close to the former ice sheets.

Observed sea-level anomalies were obtained from the European Space Agency (ESA) sea level climate change initiative (http://www.esa-sealevel-cci.org). The data set covers the period 1993–2015 and merges all the available altimeter measurements together on a regular grid with a ¼° spatial resolution (Quartly

*et al* 2017, Legeais *et al* 2018). Model simulations as well as observations have been re-gridded to a regular $1 \times 1°$ grid using bilinear interpolation.
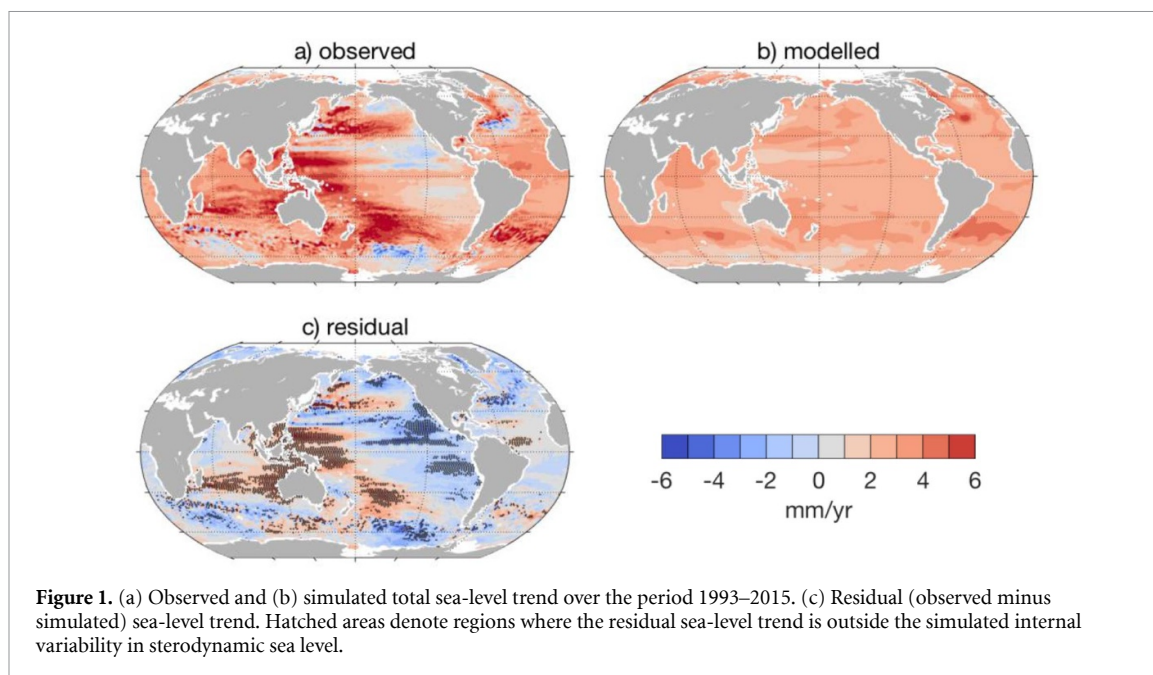
Internal variability is expected to govern spatial patterns of sea-level change at decadal time periods through ocean dynamic processes. Internal variability in free running coupled climate models is not constrained to be in phase among models or with observations. Thus, by taking the multi-model ensemble mean over 12 climate models, we are able to reduce the internal variability and better isolate the forced signal common to all models. Additionally, the magnitude and spatial pattern of internal variability in sterodynamic sea-level change is quantified for each model by computing linear trends over running 20-year periods for each grid box using the last 500 years (if available) of the fixed-forcing pre-industrial control simulation of each model. We characterise the trends that could be induced by internal variability using the 5th and 95th percentile of the resulting trend distribution and compare these percentiles to observed and ensemble-mean trends in total sea level over the period 1993–2015. In this way, we assess whether the observed trends lie within the range of simulated sterodynamic sea-level trends expected from internal variability (Richter and Marzeion 2014).

## 3. Results

In this section, we compare observed and simulated regional trends in total sea-level change, and subsequently present the individual simulated contributions and their characteristics.

The observed trend in GMSL over 1993–2015 is $2.91 \pm 0.34$ mm yr$^{-1}$ while the multi-model mean trend is $2.70 \pm 0.43$ mm yr$^{-1}$ (figure 1). The spatial variability in the observed trend pattern is much higher than in the multi-model mean (spatial standard deviation of 1.90 vs 0.58 mm yr$^{-1}$; table 1) because the internal variability is strongly reduced due to the averaging over 12 models. The spatial standard deviation of the total trend pattern based on the individual models is closer to the observed value (table 1, last column) but still underestimates the spatial variability (though within uncertainties). Common to the observed and simulated trend pattern is a larger than average rise in the mid-latitude of the western south Atlantic Ocean, east of Australia in the southern Pacific Ocean and southwest of Greenland. The spatial pattern of the residual sea-level change (observed minus model-simulated, figure 1(c)) is dominated by the observed pattern, with similar spatial variability (table 1). Over about three quarters (73%) of the world's oceans, the residual sea-level trends are within the range of internal variability in sterodynamic height, with notable exceptions in the eastern and western tropical Pacific Ocean, the southern Indian Ocean, as well as

**Figure 1.** (a) Observed and (b) simulated total sea-level trend over the period 1993–2015. (c) Residual (observed minus simulated) sea-level trend. Hatched areas denote regions where the residual sea-level trend is outside the simulated internal variability in sterodynamic sea level.

**Table 1.** Global mean sea-level trends for contributions and total sea level, spatial standard deviation of regional trend pattern for ensemble mean and mean over standard deviation of regional trend pattern from individual models (for simulated contributions). The uncertainty (in brackets) represents the standard deviation of the multi-model mean for the modelled estimates and is taken from WRCP 2018 for the observations. GSMB/ASMB Greenland/Antarctic surface mass balance, GIA glacial isostatic adjustment.
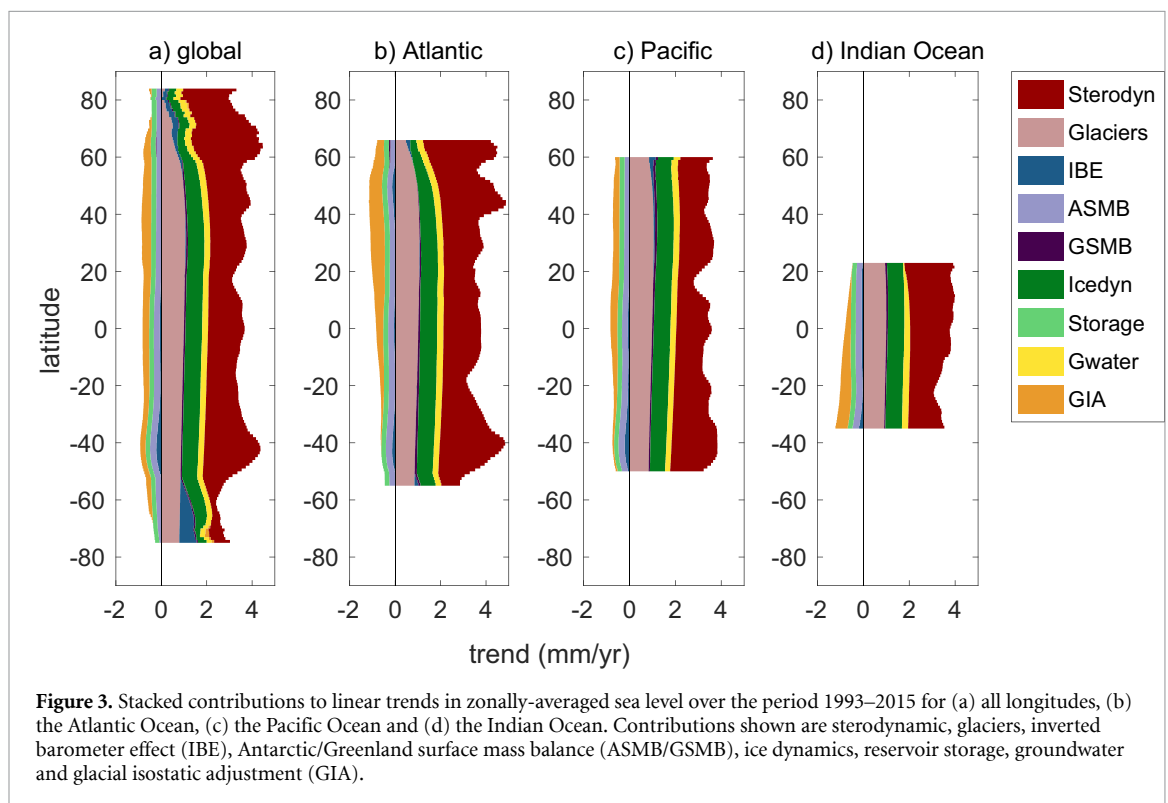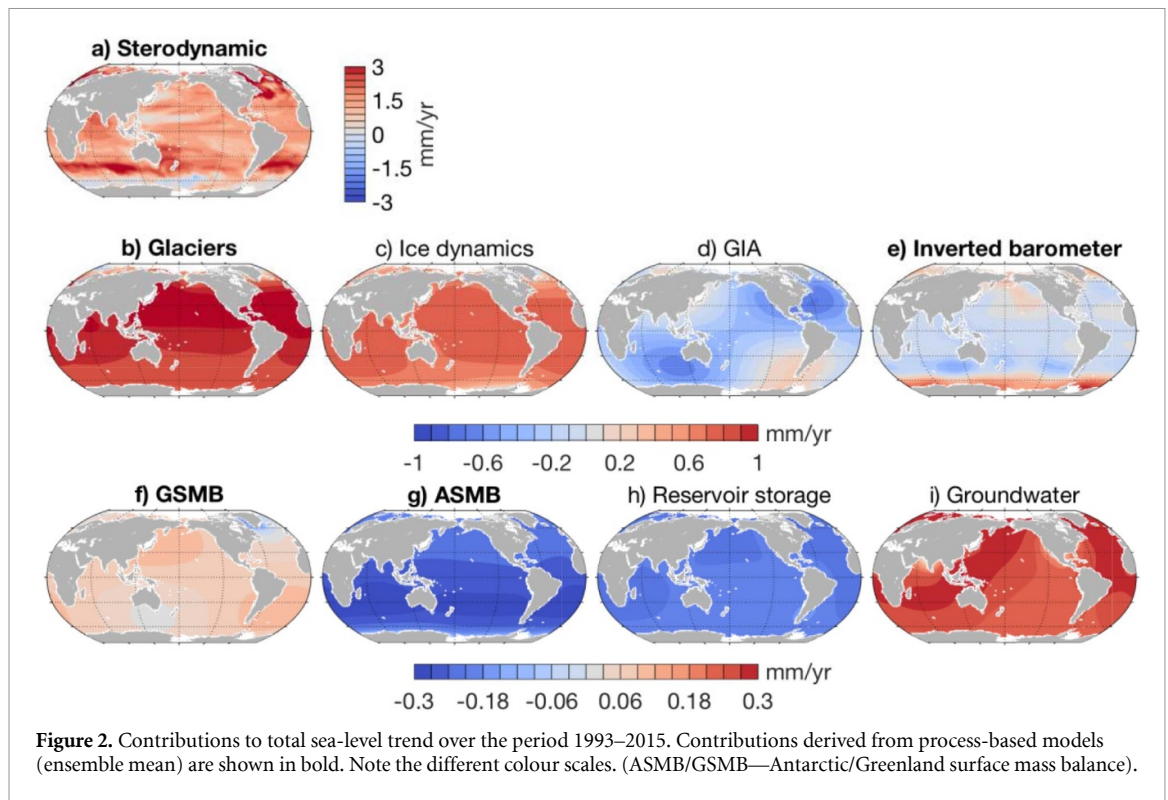
| Contribution | Global mean (mm/yr) of ensemble-mean trend | Standard deviation of (ensemble-mean) regional trend pattern (mm/yr) | Mean over standard deviation of regional trend pattern for individual models (mm/yr) |
|---|---|---|---|
| Sterodynamic | 1.48 (0.37) | 0.68 | 1.58 (0.44) |
| Glaciers | 0.93 (0.23) | 0.11 | 0.11 (0.03) |
| GSMB | 0.069 (0.05) | 0.03 | 0.03 (0.02) |
| ASMB | −0.25 (0.08) | 0.02 | 0.02 (0.01) |
| Ice dynamics | 0.69 | 0.08 | — |
| Groundwater | 0.25 | 0.03 | — |
| Reservoir storage | −0.21 | 0.01 | — |
| GIA | −0.27 | 0.22 | — |
| Inverted barometer | −0.005 (0.01) | 0.18 | 0.39 (0.14) |
| Total simulated | 2.70 (0.43) | 0.58 | 1.53 (0.44) |
| Total observed | 2.91 | 1.90 | — |
| Residual | 0.22 | 1.90 | — |

in regions of strong western boundary currents like the Kuroshio and Gulf Stream current.

The sterodynamic contribution represents the largest global contribution and dominates the spatial variability (figure 2 and table 1) away from the sources of changing land ice in the polar regions. The ensemble mean (figure 2(a)) shows distinct spatial features, e.g. a large positive sea-level trend anomaly in a zonal band between 30–60°S and a smaller than average trend south of 60°S. A larger than global-average sea-level rise is also simulated in the northern North Atlantic region. Similar to the total trend patterns, the spatial variability of the sterodynamic ensemble mean (figure 2(a)) is less than half the spatial variability of the observed sea-level trend pattern (table 1). A strong reduction is to be expected as the internal variability partly averages out in

the ensemble mean. The spatial variability of individual models (fourth column in table 1) is closer to the observed variability but still underestimates it. This may be because climate models do not represent mesoscale eddies which tend to enhance sterodynamic sea-level variability (e.g. Penduff *et al* 2010).

Glacier mass change and ice sheet dynamics constitute the second and third largest contributions to GMSL rise for the period 1993–2015. However, they contribute little to the spatial variations, except close to the changing ice masses in the polar regions. In contrast, GIA and changes in atmospheric mass loading contribute little to GMSL change but have a slightly larger effect on regional sea-level trends. The latter shows a distinct sea-level rise in the Southern Ocean along the coast of Antarctica. The regional variability of the ice sheet SMB

**Figure 2.** Contributions to total sea-level trend over the period 1993–2015. Contributions derived from process-based models (ensemble mean) are shown in bold. Note the different colour scales. (ASMB/GSMB—Antarctic/Greenland surface mass balance).



**Figure 3.** Stacked contributions to linear trends in zonally-averaged sea level over the period 1993–2015 for (a) all longitudes, (b) the Atlantic Ocean, (c) the Pacific Ocean and (d) the Indian Ocean. Contributions shown are sterodynamic, glaciers, inverted barometer effect (IBE), Antarctic/Greenland surface mass balance (ASMB/GSMB), ice dynamics, reservoir storage, groundwater and glacial isostatic adjustment (GIA).

and landwater contributions (reservoir storage and groundwater extraction) are an order of magnitude smaller than the sterodynamic contributions. Their global contributions are, however, not negligible.

Except for the polar regions, most of the simulated variability in zonally averaged sea level originates in the sterodynamic contribution while the other components contribute fairly evenly to the trend across latitudes (figure 3). In particular, the GRD fingerprints tend to represent broad spatial scales away from the source regions of ice melt. The signature of the western boundary currents is still present in the Atlantic Ocean just north of 40°N and at 40°S. In the Pacific Ocean, the variability is strongly reduced

**Figure 4.** Linear trends of observed and simulated total sea level and their residual (observed minus simulated). The red shading represents the standard deviation around the ensemble mean. The grey shading represents the ensemble mean size of internal variability in the sterodynamic contribution as derived from control simulations.
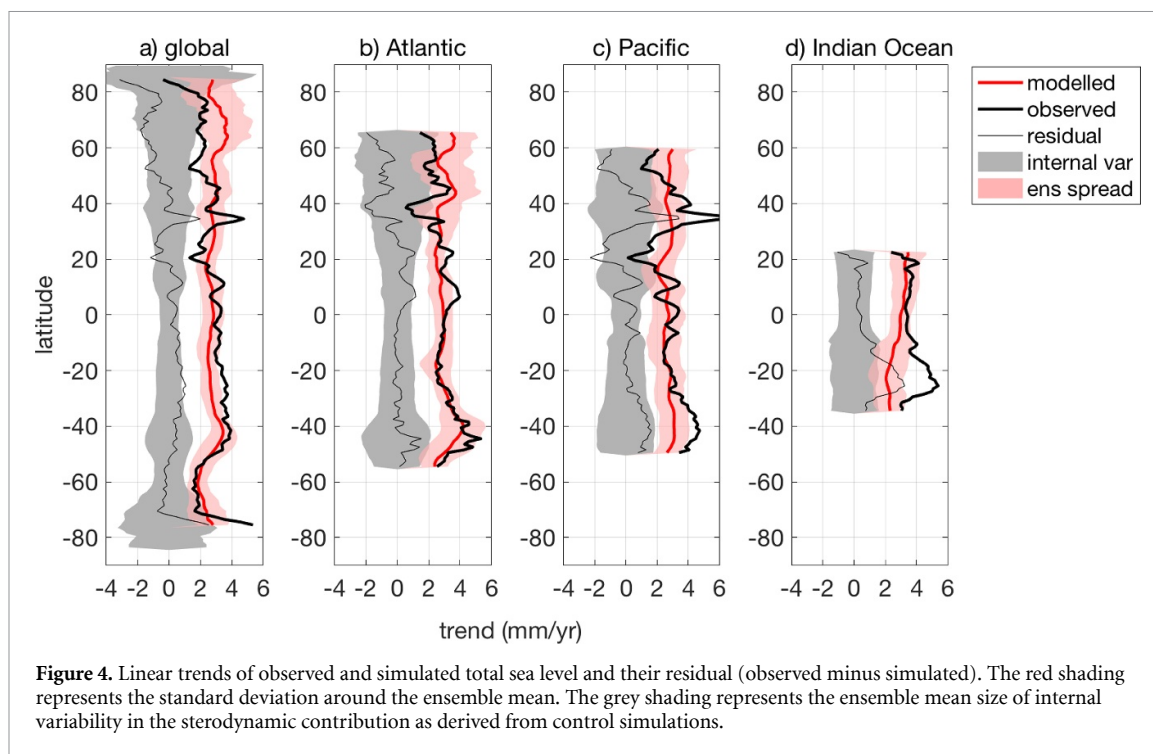
through the zonal averaging with a minimum just south of 20°N. The GRD effects lead to a reduced sea-level contribution of land ice in the polar regions: the relative importance of glacier mass change decreases significantly from the equator towards the Arctic (Antarctic peripheral glaciers are not considered), while the dynamic ice loss primarily from the Antarctic ice sheet leads to reduced trends in the Southern Ocean. GIA (geocentric part only) decreases sea level particularly in the North Atlantic as well as in the southern Indian Ocean.

Compared to the observed trends there is relatively little latitudinal variation in the simulated trends of zonally averaged sea-level change (bold black versus red line in figure 4). For the global ocean, simulated and observed zonally-averaged sea-level trends agree well, and are both outside of what would be expected from the 90% confidence interval of the simulated internal variability in sterodynamic sea level (grey envelope), except in the polar regions. The same holds for individual ocean basins (figures 4(b)–(d)) at most latitudes, confirming the presence of a forced signal in zonally averaged total sea-level change, globally as well as basin-wide.

Residual (the difference between the observed and modelled, thin lines in figure 4) trends are mostly within the range of internal variability. Simulated and observed sea-level trends agree best in the South Atlantic Ocean. The largest disagreement is found in a narrow band in the North Pacific Ocean associated with the Kuroshio extension and in a broad stretch in the Southern Indian Ocean where simulated and observed zonal trends disagree by up to 3 mm yr$^{-1}$

and the difference cannot be attributed to internal variability in sterodynamic sea level.

To test whether the forced signal originates from the GMSL rise, we removed the latter from the zonally averaged trends (figure 5). Except for localized regions in the subtropical North Pacific and southern Indian Ocean, observed as well as simulated zonal trend anomalies with respect to GMSL mostly lie within the range of internal variability. That is, the bulk of the forced signal is from the GMSL rise and regional variations in the forced signal are not detectable above the natural variability over the period 1993–2015. The spread around the ensemble mean is within the range of internal variability over the preindustrial period with an exception in the mid-latitude South Atlantic Ocean.

The analysis presented in this study has been carried out over the altimetry period 1993–2015. Recent literature has shown that the altimetry observations are subject to a bias/instrument drift in the early period during the TOPEX A mission (Watson *et al* 2015, Dieng *et al* 2017, Beckley *et al* 2017). We therefore repeated the analysis for the shorter period 1998–2015 thus excluding the TOPEX A data (supplementary material, figures 1–4 (available online at stacks.iop.org/ERL/15/094079/mmedia)). Over this shorter period of time, the discrepancy between the ensemble mean and the observations is larger as internal variability is even stronger in the observations. However, the general result is essentially the same: simulated as well as observed trends are larger than trends potentially generated from ocean internal variability.
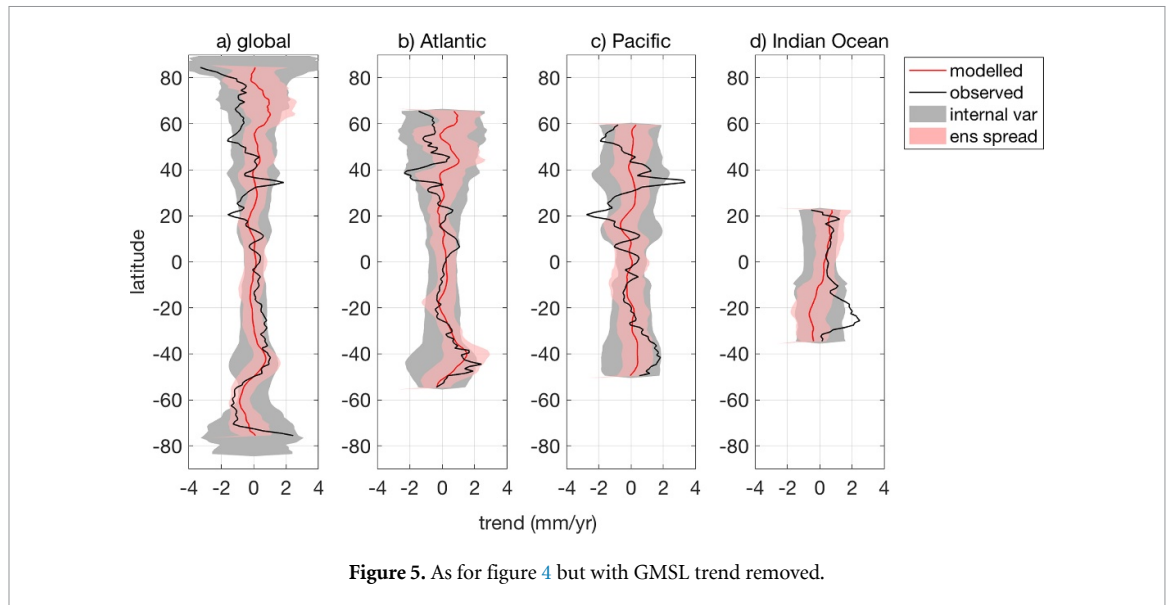
**Figure 5.** As for figure 4 but with GMSL trend removed.

## 4. Discussion

We found that the simulated spatial variability of regional sea-level trends over the period 1993–2015 is dominated by the sterodynamic contribution. Over 73% of the ocean area (unhatched area in figure 1(c)), the residual sea-level trends are within the range of estimated internal variability. This corresponds to 84% of the data (which is on a $1 \times 1°$ grid, such that the area represented by one grid point depends on the latitude), thus the disagreement constitutes only slightly more than would be expected from a 90% confidence interval (internal variability is defined as 5th to 95th percentile range). However, the individual models agree on the location of the disagreement (supplementary material figure 5) between residual sea-level trends (figure 1(c)) and internal variability. This leads to the conclusion that the disagreement is not due to pure chance but to either the inability of the models to simulate internal variability properly in some locations (mostly the tropical Pacific) or to some missing external forcing (see below).

Observed regional trends are strongly governed by internal variability over such a short time period. In this study, only internal variability originating from sterodynamic sea level is taken into consideration. Note that on the relatively short time scale considered here (decadal to just multi-decadal), internal variability generated in the ocean and the climate system is expected to be the dominant contribution to the spatial variability of sea-level change (Little *et al* 2015).

Regional sea-level residuals are unlikely to be explained by changes in the mass transfer between land and ocean because of the large spatial scales of the associated GRD fingerprints (Spada and Galassi 2016). In the regions of the western boundary currents, mesoscale-eddy activity can give rise to regional sea-level trends of several mm/yr (Sérazin *et al* 2016)

on multi-decadal time scales. This variability comes in addition to the internal variability simulated by climate models, as mesoscale eddies are not resolved by the current CMIP5 climate models (for the representation of internal variability in individual models see e.g. Landerer *et al* 2014, Palmer *et al* 2018).

The two distinct regions that show residuals that cannot be accounted for by simulated internal variability in sterodynamic sea level are the western tropical Pacific Ocean and the southern Indian Ocean. Typically, ENSO dynamics cause a see-saw trend pattern in the tropical Pacific with large sea-level rise in the western part and simultaneous sea-level drop in the eastern part and vice versa. However, the large observed sea-level rise in the western tropical Pacific Ocean cannot be accounted for by the combination of a forced signal (figure 1(b)) and internal variability in dynamic sea level. Decadal variability in the tropical Pacific Ocean is not reproduced by the models adequately (Bilbao *et al* 2015) possibly as a result of inaccurate representation of realistic wind forcing.

The misrepresentation of variability in the Pacific region might also inhibit the correct simulation of the large sea-level rise in the southern Indian Ocean. Indian Ocean sea level is subject to strong decadal variability that is governed by changes in wind stress and by changes in the Indonesian Throughflow (Han et al 2014), and therefore tightly related to changes in the tropical Pacific Ocean. Heat transport from the Pacific to the Indian Ocean started to increase abruptly in the late 1990s and is also linked to anomalous wind patterns during that period (Lee *et al* 2015).

Zonal averaging of regional sea level reduces the signature of internal variability associated with largely zonal oscillations (such as ENSO) and uncovers a distinct forced signal in model simulations as well as in observations. Particularly, in the tropical Pacific Ocean, the observed regional trends of opposite

directions cancel each other, and simulated and observed trends in zonally averaged sea level are in good agreement.

As in regional sea-level trends, there is a notable exception in the southern Indian Ocean in zonally averaged sea level. Regional sea-level trends are underestimated by climate models over the altimetry period, and the discrepancy cannot be explained by simulated internal variability in sterodynamic sea level. It is also unlikely that internal variability in the remaining contributors (land ice, land water and atmospheric pressure) has the potential to explain the large observed sea-level rise in that region.

Little is known about the internal variability of the Greenland and Antarctic ice sheet. For glaciers, Richter *et al* (2017) showed, using a slightly different subset of CMIP5 models, that the (modelled) contribution of glacier mass change to internal relative sea-level variability is small on the time scales considered here. Averaged over all latitudes, the glacier contribution to relative sea-level variability did not add more than 5% to the 20-yr linear trends originating from internal variability in the sterodynamic contribution for zonal averages. In narrow latitudinal bands in the northern North Atlantic, the contribution increases to 10% (supplementary figure 6, which is for relative sea level and based on a slightly different subset of models used in Richter *et al* 2017). To estimate the magnitude of internal variability in the mass contribution based on data used in this study, we calculated the ensemble spread of the zonally averaged mass terms around the ensemble mean over moving 22-yr windows in the simulated data over the period 1900–2015 (supplementary figures 7–9). Particularly for glaciers, the spread depends strongly on the period in time that is considered. It is generally in the order of 0.1 mm yr$^{-1}$ but increases towards 0.2 mm yr$^{-1}$ towards the end of the record. It is questionable whether this spread truly represents the magnitude of internal variability as decadal trends at this point in time depend strongly on the remaining glacier mass given their relatively small total mass. This is different for the large ice sheets as changes in the SMB during 1900–2015 hardly changed their total mass. Therefore, changes in the spread are also smaller. For the Antarctic SMB contribution, the spread is at most 0.075 mm yr$^{-1}$ at 40°S and mostly around or below 0.05 mm yr$^{-1}$ elsewhere. The spread due to the Greenland SMB is several orders of magnitudes lower. Wouters *et al* (2013) showed that the reported observed trends for the Greenland and Antarctic ice sheets (combined SMB and dynamic changes) reported by Shepherd *et al* (2012) for the period 1992–2011 are well outside the range expected from internal variability.

Recent estimates of ice-sheet mass changes show an acceleration in the contribution to sea-level change from both ice sheets (Shepherd *et al* 2018, Meredith *et al* 2019), and it is possible that we underestimate the ice sheet contribution to sea-level change with our dataset. This, however, does not affect our main conclusion that a forced signal in sea-level change can be detected at almost all latitudes in each major ocean basin.

## 5. Conclusion

We have compared total observed and simulated geocentric sea-level change over the period 1993–2015 on regional scales. We found that model-simulated and observed trends in zonally-averaged total sea level are well above what would be expected from internal variability alone. This holds for the ocean globally and for the individual ocean basins. We conclude that a forced signal can be detected at all latitudes in each major ocean basin. Further analysis shows that the forced signal stems from the global-mean sea-level rise. That is, over the period 1993–2015 the global-mean sea-level rise, up to 90% of which has been attributed to anthropogenic emissions (Slangen *et al* 2016), is detectable at each latitude in each basin. Departures from the global mean, expressed as zonal-averages, are still within simulated sterodynamic internal variability.

## Data availability statement

Data sharing is not applicable to this article as no new data were created or analysed in this study.

## ORCID iDs

Kristin Richter ⓘ https://orcid.org/0000-0002-0200-8765

Benoit Meyssignac https://orcid.org/0000-0001-6325-9843

Matthew D Palmer https://orcid.org/0000-0001-7422-198X

# References

Beckley B D, Callahan P S, Hancock D W III , Mitchum G T and Ray R D 2017 On the 'Cal-mode' correction to TOPEX satellite altimetry and its effect on the global mean sea level time series *J. Geophys. Res. Oceans* **122** 8371–84

Bilbao R A, Gregory J M and Bouttes N 2015 Analysis of the regional pattern of sea level change due to ocean dynamics and density change for 1993–2099 in observations and CMIP5 AOGCMs *Clim. Dyn.* **45** 2647–66

Chao B F, Wu Y and Li Y 2008 Impact of artificial reservoir water impoundment on global sea level *Science* **320** 212–4

Church J A and White N J 2011 Sea-level rise from the late 19th to the early 21st century *Surv. Geophys.* **32** 585–602

Dangendorf S, Hay C, Calafat F M, Marcos M, Piecuch C G, Berk K and Jensen J 2019 Persistent acceleration in global sea-level rise since the 1960s *Nat. Clim. Chang.* **9** 705–10

Dangendorf S, Marcos M, Müller A, Zorita E, Riva R, Berk K and Jensen J 2015 Detecting anthropogenic footprints in sea level rise *Nat. Commun.* **6** 1–9

Dangendorf S, Marcos M, Wöppelmann G, Conrad C P, Frederikse T and Riva R 2017 Reassessment of 20th century global mean sea level rise *Proc. Nat. Acad. Sci.* **114** 5946–51

Dieng H, Cazenave A, Meyssignac B and Ablain M 2017 New estimate of the current rate of sea level rise from a sea level budget approach *Geophys. Res. Lett.* **44** 3744–51

Döll P, Mueller Schmied H, Schuh C, Portmann F T and Eicker A 2014 Global-scale assessment of groundwater depletion and related groundwater abstractions: combining hydrological modeling with information from well observations and GRACE satellites *Water Resour. Res.* **50** 5698–720

Enderlin E M, Howat I M, Jeong S, Noh M-J, van Angelen J H and van den Broeke M R 2014 An improved mass budget for the Greenland ice sheet *Geophys. Res. Lett.* **41** 866–72

Fettweis X, Franco B, Tedesco M, Van Angelen J, Lenaerts J, Van den Broeke M and Gallée H 2013 Estimating Greenland ice sheet surface mass balance contribution to future sea level rise using the regional atmospheric climate model MAR *Cryosphere* **7** 469–89

Frieler K, Clark P U, He F, Buizert C, Reese R, Ligtenberg S R M, van den Broeke M R, Winkelmann R and Levermann A 2015 Consistent evidence of increasing Antarctic accumulation with warming *Nat. Clim. Chang.* **5** 348–52

WCRP Global Sea Level Budget Group 2018 Global sea-level budget 1993–present *Earth Syst. Sci. Data* **10** 1551–90

Gregory J M *et al* 2019 Concepts and terminology for sea level: mean, variability and change, both local and global *Surv. Geophys.* **40** 1251–89

Han W, Vialard J, Mcphaden M J, Lee T, Masumoto Y, Feng M and De Ruijter W P 2014 Indian Ocean decadal variability: a review *Bull. Am. Meteorol. Soc.* **95** 1679–703

Hay C C, Morrow E, Kopp R E and Mitrovica J X 2015 Probabilistic reanalysis of twentieth- century sea-level rise *Nature* **517** 481

Jevrejeva S, Moore J, Grinsted A, Matthews A and Spada G 2014 Trends and acceleration in global and regional sea levels since 1807 *Glob. Planet. Chang.* **113** 11–22

Landerer F W, Gleckler P J and Lee T 2014 Evaluation of CMIP5 dynamic sea surface height multi-model simulations against satellite observations *Clim. Dyn.* **43** 1271

Lee S-K, Park W, Baringer M O, Gordon A L, Huber B and Liu Y 2015 Pacific origin of the abrupt increase in Indian Ocean heat content during the warming hiatus *Nat. Geosci.* **8** 445

Legeais J-F *et al* 2018 An improved and homogeneous altimeter sea level record from the ESA Climate Change Initiative *Earth Syst. Sci. Data* **10** 281–301

Lenaerts J T, van den Broeke M R, van de Berg W J, van Meijgaard E and Munneke P K 2012 A new, high-resolution surface mass balance map of Antarctica (1979–2010) based on regional atmospheric climate modeling *Geophys. Res. Lett.* **39** L04501

Little C M, Horton R M, Kopp R E, Oppenheimer M and Yip S 2015 Uncertainty in twenty-first-century CMIP5 sea level projections *J. Clim.* **28** 838–52

Marcos M and Amores A 2014 Quantifying anthropogenic and natural contributions to thermosteric sea level rise *Geophys. Res. Lett.* **41** 2502–7

Marzeion B, Cogley J G, Richter K and Parkes D 2014 Attribution of global glacier mass loss to anthropogenic and natural causes *Science* **345** 919–21

Marzeion B, Jarosch A H and Hofer M 2012 Past and future sea-level change from the surface mass balance of glaciers *Cryosphere* **6** 1295–322

Meredith M *et al* 2019 Polar Regions *IPCC Special Report on the Ocean and Cryosphere in a Changing Climate*, ed H-O Pörtner *et al* (in preparation)

Meyssignac B *et al* 2017a Evaluating model simulations of twentieth- century sea-level rise. part ii: regional sea-level changes *J. Clim.* **30** 8565–93

Meyssignac B, Fettweis X, Chevrier R and Spada G 2017b Regional sea level changes for the twentieth and the twenty-first centuries induced by the regional variability in Greenland Ice Sheet surface mass loss *J. Clim.* **30** 2011–28

Oppenheimer M *et al* 2019 Sea level rise and implications for low-lying islands, coasts and communities *IPCC Special Report on the Ocean and Cryosphere in a Changing Climate*, ed H-O Pörtner *et al* (in preparation)

Palmer M *et al* 2018 UKCP18 marine report (https://www.metoffice.gov.uk/pub/data/weather/uk/ukcp18/science-reports/UKCP18-Marine-report.pdf)

Peltier W R 2004 Global glacial isostasy and the surface of the ice-age Earth: the ICE-5G (VM2) model and GRACE *Annu. Rev. Earth Planet. Sci.* **32** 111–49

Penduff T, Juza M, Brodeau L, Smith G C, Barnier B, Molines J-M, Treguier A-M and Madec G 2010 Impact of global ocean model resolution on sea-level variability with emphasis on interannual time scales *Ocean Sci.* **6** 269–84

Quartly G D *et al* 2017 A new phase in the production of quality-controlled sea level data *Earth Syst. Sci. Data* **9** 557–72

Ray R D and Douglas B C 2011 Experiments in reconstructing twentieth-century sea levels *Prog. Oceanogr.* **91** 496–515

Richter K and Marzeion B 2014 Earliest local emergence of forced dynamic and steric sea-level trends in climate models *Environ. Res. Lett.* **9** 114009

Richter K, Marzeion B and Riva R 2017 The effect of spatial averaging and glacier melt on detecting a forced signal in regional sea level *Environ. Res. Lett.* **12** 034004

Roberts C D, Calvert D, Dunstone N, Hermanson L, Palmer M D and Smith D 2016 On the drivers and predictability of seasonal-to-interannual variations in regional sea level *J. Clim.* **29** 7565–85

Schotman H H A 2008 Shallow-earth rheology from glacial isostasy and satellite gravity. *PhD Thesis*, TU Delft, 200 pp

Shepherd A *et al* 2012 A reconciled estimate of ice-sheet mass balance *Science* **338** 1183–118

Shepherd A, Ivins E and Rignot E *et al* 2018 Mass balance of the Antarctic Ice Sheet from 1992 to 2017 *Nature* **558** 219–22

Slangen A B, Church J A, Agosta C, Fettweis X, Marzeion B and Richter K 2016 Anthropogenic forcing dominates global mean sea-level rise since 1970 *Nat. Clim. Chang.* **6** 701–5

Slangen A B, Church J A, Zhang X and Monselesan D 2014 Detection and attribution of global mean thermosteric sea level change *Geophys. Res. Lett.* **41** 5951–9

Slangen A B *et al* 2017 Evaluating model simulations of twentieth-century sea level rise. part i: global mean sea level change *J. Clim.* **30** 8539–63

Spada G 2017 Glacial isostatic adjustment and contemporary sea level rise: an overview *Integrative Study of the Mean Sea Level and Its Components* (Berlin: Springer) pp 155–87

Spada G and Galassi G 2016 Spectral analysis of sea level during the altimetry era, and evidence for GIA and glacial melting fingerprints *Glob. Planet. Chang.* **143** 34–49

Spada G, Melini D, Galassi G and Colleoni F 2012 Modeling sea-level changes and geodetic variations by glacial isostasy: the improved SELEN code 37 (arXiv:1212.5061)

Stammer D and Hüttemann S 2008 Response of regional sea level to atmospheric pressure loading in a climate change scenario *J. Clim.* **21** 2093–101

Sutterley T C, Velicogna I, Rignot E, Mouginot J, Flament T, van den Broeke M R, van Wessem J M and Reijmer C H 2014 Mass loss of the Amundsen Sea Embayment of West Antarctica from four independent techniques *Geophys. Res. Lett.* **41** 8421–8

Sérazin G, Meyssignac B, Penduff T, Terray L, Barnier B and Molines J-M 2016 Quantifying uncertainties on regional sea level change induced by multidecadal intrinsic oceanic variability *Geophys. Res. Lett.* **43** 8151–9

Tamisiea M E 2011 Ongoing glacial isostatic contributions to observations of sea level change *Geophys. J. Int.* **186** 1036–44

Taylor K, Stouffer R and Meehl G 2012 An overview of CMIP5 and the experiment design *Bull. Am. Meteorol. Soc.* **93** 485–98

Watson C S, White N J, Church J A, King M A, Burgette R J and Legresy B 2015 Unabated global mean sea-level rise over the satellite altimeter era *Nat. Clim. Chang.* **5** 565

Wouters B, Bamber J L, Van den Broeke M R, Lenaerts J T M and Sasgen I 2013 Limits in detecting acceleration of ice sheet mass loss due to climate variability *Nat. Geosci.* **6** 613–6